JACS
JOURNAL OF THE AMERICAN CHEMICAL SOCIETY

Communication

pubs.acs.org/JACS

Rotation of a Bulky Triptycene in the Solid State: Toward Engineered Nanoscale Artificial Molecular Machines

Xing Jiang, Braulio Rodríguez-Molina, Narega Nazarian, and Miguel A. Garcia-Garibay*

Department of Chemistry and Biochemistry, University of California, Los Angeles, California 90095-1569, United States

Supporting Information

ABSTRACT: We report the design and dynamics of a solid-state molecular rotor with a large triptycene rotator. With a cross-section and surface area that are 2 and 3 times larger than those of the phenylene rotators previously studied in the solid state, it is expected that van der Waals forces and steric hindrance will render the motion of the larger triptycene more difficult. To address this challenge, we used a rigid and shape-persistent stator in a dendritic structure that reaches ca. 3.6 nm in length. Using variable-temperature solid-state ^{2}H NMR spectroscopy, we determined a symmetric three-fold rotational potential with a barrier of 10.2 kcal/mol and a pre-exponential factor of 1.1×10^{10} s^{-1}, which correspond to ca. 4600 Brownian jumps per second in the solid state at 300 K.

The development of artificial molecular machines represents a significant challenge in current science as it demands a deep understanding of the relationship between structure and dynamics, so that both characteristics can be combined to control mechanical functions resulting from molecular and supramolecular design.[1,2] Pioneering research by Mislow and co-workers in the 1980s analyzed the correlated motions of triarylmethanes and triptycene gears in solution,[3] laying the ground for the development of molecular rotors[4] capable of undergoing mechanical processes and switching functions controlled by physical and chemical stimuli.[1,2]

Considering that many macroscopic and biomolecular machines feature dense, multicomponent structures, we and others have explored some of the structural factors that enable molecular rotation in the solid state.[5,6] It is known that globular methyl groups, with a small moment of inertia and a very small van der Waals contact area, are able to undergo Brownian rotation in the GHz to THz regimes in most solids.[7] By contrast, solid-state rotation of phenylene and bicyclo[2.2.2]-octylidene groups, with larger van der Waals surfaces and more steric interactions, is not common, but it can be strongly facilitated in structures akin to macroscopic gyroscopes[5,8] with two shielding groups coaxially linked by triple bonds to the central rotator,[9] as shown in Figure 1a. Isomorphous crystals of molecular rotors **1** and **2** with triphenylsilyl stators were shown to display Brownian rotation with ambient-temperature site exchange frequencies of 9 and 110 MHz, corresponding to activation energies of 8.5 and 3.5 kcal/mol, respectively.[8] Experimental observations indicate that the size, shape, and symmetry of the rotator play very important roles in their thermal motion, pointing out that structural factors must be

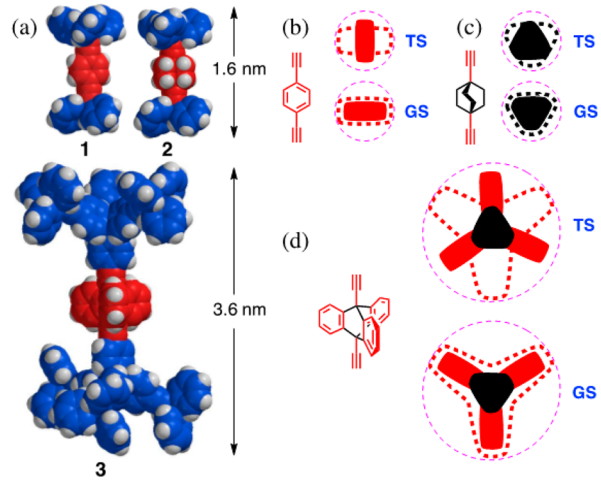

Figure 1. (a) Space-filling models of molecular rotors **1**, **2**, and **3** with 1,4-phenylene, 1,4-bicyclo[2.2.2]octylidene, and 9,10-triptycylidene rotators. The cross sections of the three rotators, of their reaction cavities, and of their volumes of revolution are represented with a filled shape, a heavy dashed line, and a thin dashed circle for (b) 1,4-phenylene, (c) 1,4-bicyclo[2.2.2]octylidene, and (d) 9,10-triptycylidene, at the ground state (GS) and rotational transition state (TS).

considered for the design of nanoscale rotors such as **3**, which may be viewed as an entry toward the design of structures of the size and complexity of ATP synthase. Thus, the different dynamics of the rotators in Figure 1 depend on the extent of the mismatch between their shapes and those of their crystal cavities at the rotational transition states (TSs). Key structural differences arise from the cross sections of the rotators, shown with filled shapes in Figure 1b–d, and those of their ground-state (GS) crystal cavities (heavy dashed lines) and volumes of revolution (thin dashed circles). While the crystal cavity is defined as the volume enclosed by the boundary formed by close neighbors,[10] the volume of revolution corresponds to the empty space that would be needed for unhindered rotation. Also shown in Figure 1 is the mismatch that occurs between the crystal cavity and the rotator at the TS.[11] Based on computer generated models, the diameter required for unhindered rotation of a triptycene group, ca. 10.7 Å, is approximately twice as large as the one needed for rotation of a phenylene or a bicyclo[2.2.2]octane, ca. 5.6 Å. It is also worth noting that the moments of inertia along their principal rotational axis for a

Received: April 9, 2014
Published: June 9, 2014

   dx.doi.org/10.1021/ja503467e | J. Am. Chem. Soc. 2014, 136, 8871–8874

methyl (3.3 g/mol·Å^2), phenylene (89 g/mol·Å^2), and bicyclo[2.2.2]octane (207 g/mol·Å^2) are 3 to 1 order of magnitude smaller than that of triptycene (1838 g/mol·Å^2).[12] In order to accommodate the larger rotator, we selected the relatively large, shape- and volume-persistent stator of molecular rotor **3** (Figure 1), which is as a higher generation dendron[13] of the stator used for **1** and **2**. We confirmed the success of this design by measuring its solid-state rotational dynamics by ^{2}H NMR.

Molecular rotor **3** and its deuterated analogue **3**-d_8 were synthesized as outlined in Scheme 1, using a divergent modular synthesis with three key building blocks consisting of 9,10-diethynyltriptycenes **6** and **6**-d_8 for the rotator and dendrimeric core, 4-iodo-4′,4″,4‴-tribromotetraphenylmethane **7** as the first-generation branch, and 3,3,3-triphenylpropyne as the surface group. Although the yields for the synthesis of intermediates **6** and **8** were modest (30% and 43%, respectively), the final coupling reaction carried out with an excess of 3,3,3-triphenylpropyne occurred in a nearly quantitative yield. All the steps indicated in Scheme 1 and the characterization of all the compounds are described in the SI. Crystallization of molecular rotor **3** by slow evaporation from several solvents led to the formation of needles with a tendency to splinter while turning opaque. Optical microscopic analysis under cross polarizers showed the initially crystalline specimens to lose their birefringence, and scanning electron microscopy (Figure 2) revealed a spontaneous splintering process. Powder X-ray diffraction (PXRD) of the resulting solids in the range of 4−50° (2θ) showed sharp peaks at 6°, 12°, and 19° (2θ) and a broad signal spanning from 3° to 33°, suggesting ordered and amorphous regions. They were shown to be chemically stable up to 573 K by differential scanning calorimetry (DSC) and thermal gravimetric analysis (TGA), making it possible to explore the rotation of the triptycene rotator using high-temperature quadrupolar echo solid-state ^{2}H NMR.[14]

Scheme 1[a]

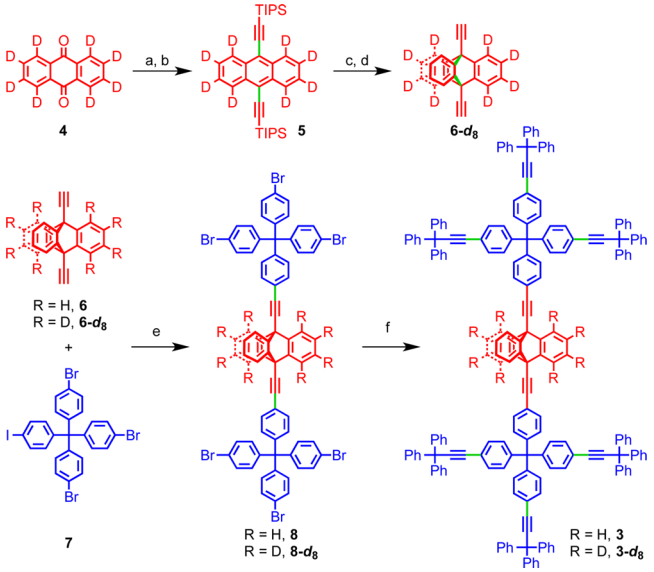

[a]Reagents and conditions: (a) TIPS acetylene, *n*-BuLi, THF, −78 °C; (b) $SnCl_2$, AcOH, EtOH, 67% over two steps; (c) anthranilic acid, isoamyl nitrite, dioxane, reflux; (d) TBAF, THF, 0 °C, 45% over two steps; (e) $PdCl_2(PPh_3)_2$, CuI, *i*-Pr_2NH, THF, reflux, 43%; (f) $PdCl_2(PPh_3)_2$, CuI, 3,3,3-triphenylpropyne, *i*-Pr_2NH, THF, reflux, 99%.

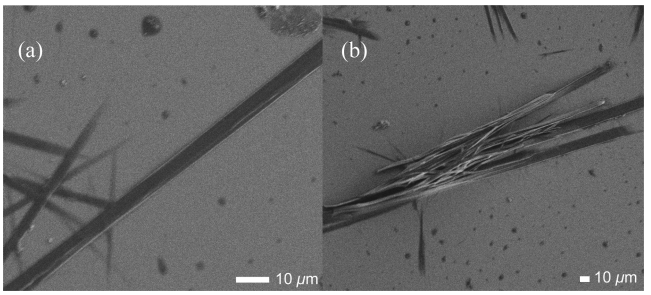

Figure 2. Scanning electron micrographs (SEM) of (a) the initial crystalline needles of **3**, which subsequently splinter into (b) fine semi-amorphous fibers.

The use of ^{2}H NMR for the determination of dynamic processes in solid-state materials relies on the predictable changes in the spectrum caused by the orientation-dependent interaction of the nuclear spin and electric quadrupole moment at the nucleus.[14] Thus, rapid (ca. 10^3−10^8 s^{-1}) variations in the orientation of the C−D bond vector with respect to the external magnetic field result in spectral changes that depend on their trajectories and frequencies. For aromatic groups undergoing axial rotation, the key parameters are the angle made between the C−D bond and the axis of rotation (cone angle) and the amplitude of the displacement between sites. As a result, the ^{2}H NMR spectrum of the partially deuterated triptycene rotator is expected to have contributions from two components, assuming a three-fold rotational potential with 120° jumps between sites (Figure 3). The deuterium atoms at the α-carbons with a C−D bond parallel to the rotational axis (cone angle 0°) do not experience any change in the ^{2}H NMR

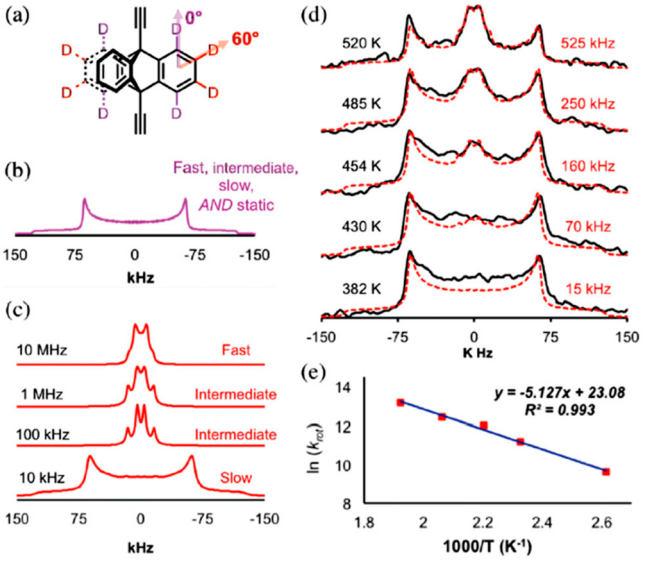

Figure 3. (a) Cone angles experienced by the tritycene C−D bonds at the α- and β-positions highlighted in purple and red, respectively. Simulated ^{2}H NMR spectra for (b) the α-C−D bonds at all exchange frequencies and (c) the β-C−D bonds assuming a three-fold symmetric rotation. (d) Superposition of experimental (black solid lines) and simulated (red dashed lines) ^{2}H NMR line shapes of rotor **3**-d_8 and (e) Arrhenius plot for the three-fold site exchange of rotor **3**-d_8.

dx.doi.org/10.1021/ja503467e | J. Am. Chem. Soc. 2014, 136, 8871−8874

spectroscopy, and their contribution to the line-shape remains unchanged as a broad Pake pattern with two sharp maxima and two shoulders (Figure 3b), regardless of the rotational rate. By contrast, deuterium atoms connected to the triptycene β-carbons make a 60° cone angle, and their contributions to the ^{2}H NMR spectrum line-shape will change as a function of rotational frequency. As shown in Figure 3c, the spectrum of deuterium atoms on β-carbons evolves from a broad Pake pattern at low temperatures, where rotational exchange rates are lower than ca. 10 kHz, to a relatively narrow pattern that changes from four to two signals as the temperature increases and the site-exchange frequency approaches motion in the fast limit at ca. 10 MHz (Figure 3c).

The ambient-temperature experimental spectrum was very similar to that of a static triptycene, indicating a rotational frequency that is ≤10 kHz. However, as shown in Figure 3d (solid lines), spectral changes were observed upon heating, with a signal developing at the center of the spectrum at ca. 430−454 K. Further heating up to 520 K, which is the limit of our solid-state NMR instrument, revealed two intense central peaks separated by 7 kHz.

Although the axial symmetry of the triptycene-d_8 rotator suggests a three-fold site exchange, the overall axial symmetry of the stators (rigorous or approximate C_3, S_3, or S_6) indicates that symmetric or unsymmetric six-fold site exchange could also account for the rotational dynamics. A simulation of symmetric three-fold rotation with an exchange frequency of 525 kHz matched the experimental spectrum at 520 K best (Figure 3d, top spectra). Considering the heterogeneous nature of the sample, a log-Gaussian distribution of exchange rates that corresponds to a Gaussian distribution of activation energies was used for the simulation with a value of $\sigma = 3$ for the width of the barrier.[15] The same procedure was applied to the simulations of the experimental spectra obtained from 485 to 382 K, and rotational frequencies were identified as 250, 160, 70, and 15 kHz, respectively. Spectral simulations with different σ values and six-fold site exchange models were explored, but they all failed to describe the experimental line shapes with the agreement observed with the three-fold site model described above.

Using the simulation-derived rotational exchange frequencies, k_{rot}, and the experimental temperatures, we built an Arrhenius plot that resulted in a good linear relationship (R^2 = 0.993). The slope and intercept correspond to an average activation energy of 10.2 kcal/mol and pre-exponential factor of ca. 1.1×10^{10} s^{-1}, respectively (Figure 3e). It should be noted that the experimental pre-exponential factor is about an order of magnitude smaller than the value expected for rotational inertia, 5.6×10^{11} s^{-1},[12] as observed for solids with limited long-range order. These activation parameters indicate that triptycene rotation at ambient temperature (300 K) should occur with a frequency of 4.6 kHz, which corresponds to jumps between sites every 220 μs. It is notable that, despite the many conformations that could be adopted by the stator to make a more complex rotational potential, the ^{2}H NMR spectral simulations clearly indicate a three-fold symmetric potential with ca. 120° jumps per second between sites. We interpret this as an indication that the potential energy profile is primarily determined by the relatively large triptycene rotator.

In conclusion, an expanded triptycene rotator in molecular rotor **3** can be rendered functional in the context of a volume-conserving system by using a stator that consists of relatively large, shape- and volume-persistent dendrons. A very efficient divergent but modular strategy was successfully implemented in order to overcome the challenges involved in the coupling of bulky stator groups onto the central triptycene rotator. Using variable-temperature solid-state ^{2}H NMR spin−echo experiments and line shape analysis, we showed that rotation in the intermediate exchange regime occurs in the range of 382−520 K with an average activation energy of 10.2 kcal/mol and a pre-exponent of 1.1×10^{10} s^{-1}. These results confirm that mechanical functions in solids can be attained for larger molecules by suitable molecular design and bode well for in the nascent field of artificial molecular machines. The success reported in this paper with a large, star-shaped rotator suggests structural strategies for the design of gearing motions in condensed solid phases.[16]

■ ASSOCIATED CONTENT

Supporting Information

Detailed syntheses and characterization of new compounds; solid-state CPMAS and ^{2}H NMR characterization. This material is available free of charge via the Internet at http://pubs.acs.org.

■ AUTHOR INFORMATION

Corresponding Author

mgg@chem.ucla.edu

Notes

The authors declare no competing financial interest.

■ ACKNOWLEDGMENTS

This work was supported by National Science Foundation grant DMR1101934. We thank Dr. Antoine Stopin for help with the SEM images.

■ REFERENCES

(1) (a) Coskun, A.; Banaszak, M.; Astumian, R. D.; Stoddart, J. F.; Grzybowski, B. A. *Chem. Soc. Rev.* **2012**, *41*, 19. (b) Kay, E.; Leigh, D.; Zerbetto, F. *Angew. Chem., Int. Ed.* **2007**, *46*, 72.

(2) (a) Lewandowski, B.; De Bo, G.; Ward, J. W.; Papmeyer, M.; Kuschel, S.; Aldegunde, M. J.; Gramlich, P. M. E.; Heckmann, D.; Goldup, S. M.; D'Souza, D. M.; Fernandes, A. E.; Leigh, D. A. *Science* **2013**, *339*, 189. (b) Perera, U. G. E.; Ample, F.; Kersell, H.; Zhang, Y.; Vives, G.; Echeverria, J.; Grisolia, M.; Rapenne, G.; Joachim, C.; Hla, S.-W. *Nat. Nanotechnol.* **2013**, *8*, 46. (c) Nguyen, T.-T.-T.; Türp, D.; Wagner, M.; Müllen, K. *Angew. Chem., Int. Ed.* **2013**, *52*, 669. (d) Schmittel, M.; De, S.; Pramanik, S. *Angew. Chem., Int. Ed.* **2012**, *51*, 3832. (e) Carroll, G. T.; Pollard, M. M.; van Delden, R.; Feringa, B. L. *Chem. Sci.* **2010**, *1*, 97. (f) Silvi, S.; Arduini, A.; Pochini, A.; Secchi, A.; Tomasulo, M.; Raymo, F. M.; Baroncini, M.; Credi, A. *J. Am. Chem. Soc.* **2007**, *129*, 13378.

(3) Iwamura, H.; Mislow, K. *Acc. Chem. Res.* **1988**, *21*, 175.

(4) (a) Comotti, A.; Bracco, S.; Ben, T.; Qiu, S.; Sozzani, P. *Angew. Chem., Int. Ed.* **2014**, *53*, 1043. (b) Tierney, H. L.; Murphy, C. J.; Jewell, A. D.; Baber, A. E.; Iski, E. V.; Khodaverdian, H. Y.; McGuire, A. F.; Klebanov, N.; Sykes, E. C. H. *Nat. Nanotechnol.* **2011**, *6*, 625. (c) Akutagawa, T.; Endo, D.; Kudo, F.; Noro, S.; Takeda, S.; Cronin, L.; Nakamura, T. *Cryst. Growth Des.* **2008**, *8*, 812. (d) Nawara, A. J.; Shima, T.; Hampel, F.; Gladysz, J. A. *J. Am. Chem. Soc.* **2006**, *128*, 4962. (e) Kottas, G. S.; Clarke, L. I.; Horinek, D.; Michl, J. *Chem. Rev.* **2005**, *105*, 1281. (f) Hiraoka, S.; Shiro, M.; Shionoya, M. *J. Am. Chem. Soc.* **2004**, *126*, 1214.

(5) (a) Vogelsberg, C. S.; Garcia-Garibay, M. A. *Chem. Soc. Rev.* **2012**, *41*, 1892. (b) Khuong, T.-A. V.; Nuñez, J. E.; Godinez, C. E.; Garcia-Garibay, M. A. *Acc. Chem. Res.* **2006**, *39*, 413.

(6) (a) Comotti, A.; Bracco, S.; Ben, T.; Qiu, S.; Sozzani, P. *Angew. Chem., Int. Ed.* **2014**, *53*, 1043. (b) Setaka, W.; Yamaguchi, K. *J. Am.*

Chem. Soc. **2013**, *135*, 14560. (c) Akutagawa, T.; Shitagami, K.; Nishihara, S.; Takeda, S.; Hasegawa, T.; Nakamura, T.; Hosokoshi, Y.; Inoue, K.; Ikeuchi, S.; Miyazaki, Y.; Saito, K. *J. Am. Chem. Soc.* **2005**, *127*, 4397.

(7) (a) Wang, X.; Beckmann, P. A.; Mallory, C. W.; Rheingold, A. L.; DiPasquale, A. G.; Carroll, P. J.; Mallory, F. B. *J. Org. Chem.* **2011**, *76*, 5170. (b) van der Putten, D.; Diezman, G.; Fujara, F.; Hartmann, K.; Silescu, H. *J. Chem. Phys.* **1992**, *96*, 1748. (c) Rodriguez-Molina, B.; Perez-Estrada, S.; Garcia-Garibay, M. A. *J. Am. Chem. Soc.* **2013**, *135*, 10388.

(8) Karlen, S. D.; Reyes, H.; Taylor, R. E.; Khan, S. I.; Hawthorne, M. F.; Garcia-Garibay, M. A. *Proc. Natl. Acad. Sci. U.S.A.* **2010**, *107*, 14973.

(9) As proposed in ref 4c, we use the word "rotor" to describe the entire molecular assembly, and "rotator" and "stator" to denote the rotary units and the static component, respectively.

(10) Cohen, M. D. *Angew. Chem., Int. Ed.* **1975**, *14*, 386.

(11) Rotational motion in the case of **1** relies on transient deformations of the crystal cavity: Khuong, T.-A. V.; Dang, H.; Jarowski, P. D.; Maverick, E. F.; Garcia-Garibay, M. A. *J. Am. Chem. Soc.* **2007**, *129*, 839.

(12) (a) Moments of inertia were determined on minimized structures using the ChemPropStd function in SC ChemDraw 3D Pro.. (b) Inertial rotational frequency $\tau_{IR} - 1$ can be estimated from the moment of inertia (I) of a rotator using the equation $\tau_{IR} - 1 = [(2\pi/9)(I/k_BT)^{1/2}]^{-1}$. The values for methyl, phenylene, bicyclo[2.2.2]octane, and triptycene groups are 1.3×10^{13}, 2.4×10^{12}, 1.6×10^{12}, and 5.6×10^{11} s^{-1}, respectively. Please see: Kawski, A. *Crit. Rev. Anal. Chem.* **1993**, *23*, 459.

(13) (a) Bauer, R. E.; Grimsdale, A. C.; Müllen, K. *Top. Curr. Chem.* **2005**, 253. (b) Moore, J. S. *Acc. Chem. Res.* **1997**, *30*, 402.

(14) Macho, V.; Brombacher, L.; Spiess, H. W. *Appl. Magn. Reson.* **2001**, *20*, 405.

(15) (a) Schmidt, C.; Kuhn, J.; Spiess, H. W. *Prog. Colloid Polym. Sci.* **1985**, *71*, 71−76. (b) Fischer, E. W.; Hellmann, G. P.; Spiess, H. W.; Hörth, F. J.; Gearius, U.; Wehrle, M. *Makromol. Chem. Suppl.* **1985**, *12*, 189−214.

(16) For a recent example reporting geared motion in the solid state, see: Lemouchi, C.; Iliopoulos, K.; Zorina, L.; Simonov, S.; Wzietek, P.; Cauchy, T.; Rodríguez-Fortea, A.; Canadell, E.; Kaleta, J.; Michl, J.; Gindre, D.; Chrysos, M.; Batail, P. *J. Am. Chem. Soc.* **2013**, *135*, 9366.